Chapter XV
Accuracy Bounds for Wireless Localization Methods

Michael L. McGuire
University of Victoria, Canada

Konstantinos N. Plataniotis
University of Toronto, Canada

ABSTRACT

Node localization is an important issue for wireless sensor networks to provide context for collected sensory data. Sensor network designers need to determine if the desired level of localization accuracy is achievable from their network configuration and available measurements. The Cramér-Rao lower bound is used extensively for this purpose. This bound is loose since it uses only information from measurements in its calculations. Information, such as that from the sensor selection process, is not considered. In addition, non-line-of-sight radio propagation causes the regularity conditions of the Cramér-Rao lower bound to be violated. This chapter demonstrates the Weinstein-Weiss and extended Ziv-Zakai lower bounds for localization error which remain valid with non-line-of-sight propagation. These bounds also use all available information for bound calculations. It is demonstrated that these bounds are tight to actual estimator performance and may be used determine the available accuracy of location estimation from survey data collected in the network area.

INTRODUCTION

To provide context for data collected by wireless sensor networks, it is necessary for the sensor network to supply accurate location information for its component sensor nodes (Sheu et al. 2006). To this end, several algorithms and sensor types have been developed for sensor node localization in these networks (Patwari et al. 2003; Ray et al. 2006). These proposed localization systems have been shown to provide excellent localization accuracy for the sensor nodes and mobile terminals in these networks.

The remainder of this book describes the design and use of several of these algorithms. However, an important issue for a network designer is to determine what sensors and network topologies are required to achieve the necessary level of localization accuracy for their application. To make these design decisions, tools are required for analytically evaluating the performance of different localization systems with different sensor positions.

The purpose of this chapter is to describe tools for the accuracy analysis of localization systems for wireless sensor networks. The chapter will focus on localization systems based on base stations at known positions making measurements of the radio signals from the sensor nodes. It should be noted that while this chapter describes only radio-based measurements for localization within sensor networks, the mathematical tools are easily applied to other measurements such as acoustic-based distance measurements.

Evaluation methods for localization systems serve two purposes. First, they allow a network designer, prior to the creation of the senor network, to obtain a quantitative bound on how well the localization of sensor nodes can be performed with given types of localization measurements and with different geometric arrangements of the measuring base stations. A network designer can then determine which of a set of possible network designs will achieve the required localization accuracy for their application. Second, these tools can be used to evaluate the performance of an existing localization system to see if all the potential location accuracy is being achieved or if further improvements are possible. The tools help to quantify the cost and accuracy tradeoffs of different component choices in a localization system's design.

In the radiolocation literature, there have been several figures of merit proposed for localization accuracy such as the Circular Error Probable (CEP) and the Geometric Dilution of Precision (GDOP) (Torrieri 1984; Tekinay et al. 1998). These figures of merit provide useful information for the analysis of the performance of location systems, but these values are difficult to calculate for localization systems coping with multipath or non-line-of-sight (NLoS) radio propagation. In Line-of-Sight (LoS) radio propagation, radio signals travel directly on the shortest straight line path from the node to be located to the measuring base stations, whereas during NLoS radio propagation this path is obstructed and the signal is reflected and diffracted during propagation from the target node to the measuring base stations. NLoS propagation complicates the localization problem since the signal characteristics are not only a function of the node and base station locations but also a function of the location of obstructions in the propagation environment.

To provide accuracy information for localization in the presence of multipath and NLoS propagation, figures of merit have been derived in the localization literature such as the Cramér-Rao lower bound on the mean square error of the location estimates. The local Cramér-Rao lower bound has been derived for localization in the presence of multipath and random NLoS radio propagation and used to evaluate the performance of many localization systems (Qi et al. 2002; Botteron et al. 2004). This bound provides an excellent method of evaluating the effects of the locations of the base stations and measurement noise levels on localization accuracy. A difficulty with the use of the Cramér-Rao lower bound as a general evaluation tool for localization accuracy is that it considers the current radio signal measurements as the only source of information on node location. In other words, the Cramér-Rao lower bound assumes that the node location is a deterministic value and the localization system has no other information about the node location prior to the measurements. Other sources of information, such as the sensor selection procedure or the measurements taken in the past, are not considered, so the Cramér-Rao lower bound is no longer a valid lower bound for localization systems where this information is available.

An extension of the Cramér-Rao lower bound, known as the Bayesian Cramér-Rao lower bound, has been developed to manage information other than that contained in the measurements about the node's location. The additional information is modeled as generating a probability density function for a node's location prior to the availability of the measurements. Unfortunately, the Bayesian Cramér-Rao lower bound has several regularity conditions that are violated for the node localization scenarios of greatest interest. This chapter addresses this problem by demonstrating how the more general Weinstein-Weiss lower bound (Weinstein and Weiss 1988) and the Extended Ziv-Zakai lower bound (Bell et al. 1997) are applied to the node localization problem. The chapter demonstrates the use of these bounds for considering the effect of sensor selection on the localization error bounds. It is demonstrated how, with the use of a motion model, a lower bound is calculated for the localization of nodes that are in motion. This chapter also shows how the Extended Ziv-Zakai bound is used with a measurement survey data set collected in a wireless sensor network's environment to determine a measure of what localization accuracy is attainable for the wireless sensor network at different noise levels.

The rest of this chapter is organized as follows. The next section gives a brief summary of the signal models used in this chapter. The mathematical notation for the chapter is also presented. The third section of the chapter contains a review of the evaluation methods for localization of nodes when the nodes have deterministic locations. The concepts of the CEP and GDOP are reviewed and explained. The fourth section of the chapter describes the Cramér-Rao lower bound on terminal localization from radio measurements. The effects of sensor geometry on propagation distance measurements and the received signal measurements are discussed. The fifth section of the chapter describes the integration of prior information on node location into the bound calculations. The Bayesian Cramér-Rao lower bound is described and the difficulties with its application to node localization are noted. The more general bounds on terminal location, the Weinstein-Weiss and extended Ziv-Zakai bounds, are then introduced. The sixth section of the chapter provides examples of the lower bound calculations with a summary of how the bounds described in previous sections are calculated for a sample network. The last section of the chapter presents the conclusions of the chapter with an overview of the results.

MEASUREMENT AND SIGNAL MODEL

In this chapter, vectors are denoted with bold lower case letters and matrices are denoted with bold upper case letters. Subscripts are used to index the entries of matrices and vectors so $\mathbf{v}_i$ is referring to the i^{th} entry of vector **v**, while $C_{i,j}$ is the j^{th} entry of the i^{th} row of the matrix **C**. Many of the variables in this chapter are random and they are specified in terms of their probability density functions. The function $f(\mathrm{x})$ is the probability density function of the random vector **x**, and $f(\mathrm{x} \mid \mathrm{y})$ is the conditional probability density function of random vector **x** given the value of random vector **y**.

This chapter demonstrates how to calculate bounds for node localization from radio received signal strength (RSS), time of arrival (ToA), time difference of arrival (TDoA), or angle of arrival (AoA) measurements. In this paper, the terms node and terminal are used interchangeably. These measurements were selected since they are the most popular radio signal measurements for wireless node localization. The methods described for calculations of lower bound on localization error are applicable to other measurements that have been proposed for node localization, such as acoustic distance measurements or radio impulse response matching.

The node location at sample time k is specified by the vector $\boldsymbol{\theta}(k) = [\,p_x(k)\;p_y(k)]^T$ where $(p_x(k), p_y(k))$ are the x and y coordinates of the node of interest. This chapter concentrates on two dimensional localizations. The presented bound calculations are easily generalized to three dimensional localizations, if required. The measurement vector for sample time k is denoted as $\mathbf{z}(k)$. The node localization is performed with measurements from m fixed location base stations at known locations. In wireless sensor networks, the base stations are either localized by measurements made at the time the sensor network is setup or these nodes are equipped with Global Position System (GPS) receivers.

For RSS, ToA, or AoA measurements, the i^{th} entry of the measurement vector is given by

$$\mathbf{z}_i(k) = \mathrm{m}[\boldsymbol{\theta}(k), \mathbf{b}^i] + \mathbf{n}_i(k) \tag{1}$$

where $\mathrm{m}[\boldsymbol{\theta}(k), \mathbf{b}^i]$ gives the noise free measurement for radio propagation from location $\boldsymbol{\theta}(k)$ to the i^{th} base station's location specified by the vector $\mathbf{b}^i$, and $\mathbf{n}_i(k)$ is the i^{th} entry of the measurement noise vector $\mathbf{n}(k)$. To simplify later calculations, the time measurement for the ToA measurement is converted to a distance measurement by multiplication of the measurement by the radio signal propagation speed.

The measurement function for unobstructed LoS propagation is specified by

$$\mathrm{m}[\boldsymbol{\theta}(k), \mathbf{b}^i] = \begin{cases} 10\alpha \log_{10} \left\| \boldsymbol{\theta}(k) - \mathbf{b}^i \right\| & \text{RSS measurement (dB)} \\ \left\| \boldsymbol{\theta}(k) - \mathbf{b}^i \right\| & \text{ToA measurement (m)} \\ \angle[\boldsymbol{\theta}(k) - \mathbf{b}^i] & \text{AoA mesurement (radians)} \end{cases} \tag{2}$$

with $\|\mathbf{v}\|$ being the Euclidean length of vector $\mathbf{v}$, and α being the radio pathloss propagation constant varying from 2 to 4 in urban environments, and the $\angle[\boldsymbol{\theta}(k) - \mathbf{b}^i]$ operator gives the angle of the difference vector $\mathbf{Q}(k)$-$\mathbf{b}^i$ (Steele 92). It is assumed for ToA measurements that the time of signal transmission from the source is known. For TDoA measurements, each entry of the measurement vector is the difference between the propagation times for the measuring base station and the reference base station. Therefore, the TDoA measurement vector is calculated from a ToA measurement vector as $\mathbf{z}^{\text{TDoA}}(k) = \mathbf{F}\,\mathbf{z}^{\text{ToA}}(k)$ where, without loss of generality, if base station 1 is the reference base station then $\mathbf{F} = [-\mathbf{1}^{m-1} \quad \mathbf{I}^{m-1}]$ with $\mathbf{1}^{m-1}$ being an $(m-1)\times 1$ vector with all one entries and $\mathbf{I}^{m-1}$ being an $(m-1)\times(m-1)$ identity matrix.

The measurement noise for RSS, ToA, and AoA measurements is usually specified as a zero mean Gaussian random vector with a covariance matrix given by $\mathrm{Var}[\mathbf{n}(k)] = \mathbf{C}$. If this is the case, the measurement noise vector for TDoA measurements is a zero mean vector of length *m-1* with a covariance given by $\mathbf{C}^{\text{TDoA}} = \mathbf{F}\mathbf{C}^{\text{ToA}}\mathbf{F}^T$.

These measurement equations are only provided to assist with the description of the examples later in the chapter. The lower bound methods described in this chapter are not dependent on these propagation equations.

EVALUATION OF LOCALIZATION ACCURACY FOR NODES WITH DETERMINISTIC LOCATIONS

The node localization problem is specified as computing an estimate of the mobile terminal location at time k based on the measurements taken at time k:

$$\hat{\boldsymbol{\theta}}(k) = \mathrm{e}[\mathbf{z}(k)]\cdot \tag{3}$$

$\hat{\boldsymbol{\theta}}(k) = [\hat{p}_x(k)\ \hat{p}_y(k)]^T$ is the estimated location at sample interval k. $\mathrm{e}[\mathbf{z}(k)]$ is an estimator function which maps from measurements to estimated locations. The reader is referred to the remainder of this volume for more details on how to implement these functions. This chapter instead focuses on figures of merit and bounds on the accuracy of these functions for several measurement types.

Figures of merit that have been proposed in the previous literature for stationary target localization are the Mean Distance Error (MDE), the Mean Square Error (MSE), the Root Mean Square Error (RMSE), the Geometric Dilution of Precision (GDOP), and the Circular Error Probable (CEP) (Torrieri 1984; Tekinay et al. 1998). These figures of merit quantify the uncertainty in the localization when the mobile terminal location is at a given point. The most commonly used figures or merit for stationary target location accuracy are the Mean Distance Error (MDE), Mean Square Error (MSE), and Root Mean Square Error (RMSE). These figures of merit give quantitative values to specify the magnitude of localization errors. The MDE is the mean distance of the estimated terminal location from the true mobile terminal location: $\mathrm{MDE}(k) = \mathrm{E}\left\{\sqrt{[p_x(k)-\hat{p}_x(k)]^2+[p_y(k)-\hat{p}_y(k)]^2}\right\}$ where $\mathrm{E}[\bullet]$ is the statistical expectation operator. The MSE is the mean squared distance of the estimated terminal location from the true mobile terminal location: $\mathrm{MSE}(k) = \mathrm{E}\{[p_x(k)-\hat{p}_x(k)]^2+[p_y(k)-\hat{p}_y(k)]^2\}$. RMSE is simply the square root of MSE: $\mathrm{RMSE}(k) = \sqrt{\mathrm{MSE}(k)}$. The advantage of MDE is that its value is easily mapped to useful performance measures in the localization application domain. However, MDE is unfortunately difficult to calculate in analysis of estimation algorithms. Conversely, the MSE is easily calculated in theoretical work but has less correspondence to real world distances. As a compromise, RMSE is often used as figure of merit. RMSE is easily calculated and its value is significant to field applications since it can be easily shown that RMSE is always greater than MDE:

$$
\begin{array}{rccc}
 & \mathrm{Var}[\mathrm{MDE}(k)] & \geq & 0 \\
\Rightarrow & \mathrm{MSE}(k)-[\mathrm{MDE}(k)]^2 & \geq & 0 \\
\Rightarrow & \mathrm{MSE}(k) & \geq & [\mathrm{MDE}(k)]^2 \\
\Rightarrow & \mathrm{RMSE}(k) & \geq & \mathrm{MDE}(k).
\end{array}
\tag{4}
$$

where $\mathrm{Var}[\bullet]$ is the statistical variance operator. This is a useful result for performance bound purposes, since bounds on RMSE are easily calculated from bounds on MSE.

Due to non-linearity in the relationship between the mobile terminal locations and the available measurement vectors, the magnitude of the location error is dependent on the relative location of the mobile terminal to the measuring base stations (Spirito 2001). The Geometric Dilution of Precision (GDOP) figure of merit is useful in the analysis of the location dependence in the localization error. GDOP is defined as the ratio of RMSE error over the standard deviation of the measurement errors, given by, using the definition from (Torrieri 1984):

$$
\mathrm{GDOP} = \frac{\mathrm{RMSE}}{\sqrt{\mathrm{Var(measurement\ noise)}}}\ . \tag{5}
$$

GDOP allows for the uncertainty when the mobile is at different positions relative to the base stations to be specified relative to the variance of the available measurements. GDOP is useful when evaluating the choices of different measuring nodes for a given location system. A high GDOP indicates the geometry of measuring base station positions is inappropriate for accurate localization.

The mobile terminal localization error can be decomposed into two parts: a bias which is a fixed localization error vector resulting from the non-linearity in the relationship from measurement to location, and a random localization error vector. Circular Error Probable (CEP) provides quantitative values for the magnitude of the random portion of the localization error. CEP is defined as the radius of the circle which, for a given true location of the mobile terminal, contains half of the estimated locations of the mobile terminal (Torrieri 1984; Tekinay et al. 1998). This is illustrated in Figure 1. These figures of merit have been extensively studied in the case for line-of-sight (LoS), single path radio propagation and several useful results are available (Torrieri 1984). However, in more general cases, other figures of merit are required. The next subsection describes the use of lower bounds on localization error as figures of merit.

THE CRAMÉR-RAO BOUND ON TERMINAL LOCALIZATION ERROR

One factor that is lacking in the evaluation methods described in the previous section is that they do not give an indication of how much improvement is possible in a given mobile terminal localization system. This section describes methods for calculating bounds on the localization errors. The performance of any localization system cannot be better than these lower bound values. These bounds can be used as an indication of how much improvement can be made to a given estimator or how close a localization system is to providing optimal performance.

Another purpose for deriving these bounds is that they give a quantifiable measurement of how much information a single measurement vector, $\mathbf{z}(k)$, contains about the location of the mobile terminal. This information measure is needed for the derivation of the bounds on the localization error for time filtering of localization measurements provided later in this chapter.

A classification of some commonly used bounds for parametric estimation problems is given in Table 1. The Cramér-Rao bound gives a lower bound on the MSE of estimators of a deterministic parameter (Kay 1993). Cramér-Rao bounds have been derived for these performance measures for location estimates using ToA and TDoA measurements (Spirito 2001; Qi and Kobayashi 2002; Botteron et al. 2004). It should be noted that the bound in (Spirito 2001) is identical to the standard Cramér-Rao lower bound without using the standard Cramér-Rao lower bound derivation (Kay 1993). The standard Cramér-Rao bound gives a lower bound on the MSE of unbiased localization when the node is at a given location $\theta(k)$:

Figure 1. Circular error probable (CEP) definition

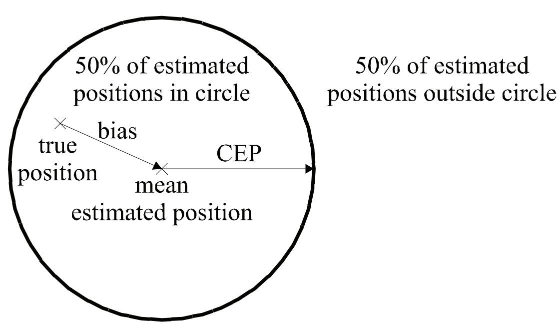

Table 1. Partial taxonomy of estimator lower bounds

Deterministic θ(*k*)		Random θ(*k*) (Bayesian Estimation)	
Restrictions on *f*(**z**(k) | θ(*k*))	Bound	Restrictions on *f*(**z**(k), θ(*k*))	Bound
None	Barankin (Rife et al., 1975)	None	Weiss-Weinstein (Weinstein and Weiss1988) Extended Ziv-Zakai (Bell et al. 1997)
Twice differentiable w.r.t. elements of θ(*k*)	Cramér-Rao (Kay 1993)	Twice differentiable w.r.t. elements of θ(*k*)	Bayesian Cramér-Rao (Van Trees 2001)

$$\mathrm{E}\{[p_x(k)-\hat{p}_x(k)]^2+[p_y(k)-\hat{p}_y(k)]^2\mid \boldsymbol{\theta}(k)\}\geq\{\mathbf{J}[\boldsymbol{\theta}(k)]\}^{-1}{}_{1,1}+\{\mathbf{J}[\boldsymbol{\theta}(k)]\}^{-1}{}_{2,2}\,, \tag{6}$$

where $\mathbf{J}[\boldsymbol{\theta}(k)]$ is defined as

$$\mathbf{J}[\boldsymbol{\theta}(k)]=-\mathrm{E}\left\{\nabla_{\boldsymbol{\theta}(k)}\left[\nabla_{\boldsymbol{\theta}(k)}\log\Big(f\big(\mathbf{z}(k)\big|\boldsymbol{\theta}(k)\big)\Big)\right]^T\big|\boldsymbol{\theta}(k)\right\} \tag{7}$$

with $f(\mathbf{z}(k)\,|\,\boldsymbol{\theta}(k))$ being the conditional probability density function of the measurement vector **z**(*k*) given the true location **θ**(*k*) during sample interval *k*. E[x | y] is the conditional expectation operator. The ∇ operator is defined as

$$\nabla_{\mathbf{v}}=\left[\frac{\partial}{\partial\mathbf{v}_1},\frac{\partial}{\partial\mathbf{v}_2},\cdots,\frac{\partial}{\partial\mathbf{v}_n}\right]. \tag{8}$$

The matrix $\mathbf{J}[\boldsymbol{\theta}(k)]$ is the Fisher information matrix of the locations given the measurements.

For the Cramér-Rao lower bound to be valid, certain necessary 'regularity' conditions must be satisfied. These 'regularity' conditions are that the partial derivatives within (7) exist and that the expectations are bounded. For the localization problem, this is equivalent to the requirement that

$$\mathrm{E}\{\nabla_{\boldsymbol{\theta}(k)}\log[f(\mathbf{z}(k)\,|\,\boldsymbol{\theta}(k))]\,|\,\boldsymbol{\theta}(k)\}^T=\begin{bmatrix}0\\0\end{bmatrix} \tag{9}$$

for all **θ**(*k*) (Kay, 1993). Because of these conditions, many of the bounds presented in the localization literature are based on three assumptions that are not unconditionally true in many environments of interest (Spirito 2001; Botteron et al. 2004). Each of these assumptions is addressed below.

1. **Radio propagation is line-of-sight to the node.** The LoS propagation assumption is used to derive $f(\mathbf{z}(k)\,|\,\boldsymbol{\theta}(k))$ functions. The LoS assumption means the conditional probability density function value for **z**(*k*) is dependent only on mobile terminal and measuring base station positions. The assumption of LoS propagation is not always satisfied in urban or indoor environments. NLoS propagation measurements are dependent on the position of buildings and other geographic features in the propagation environment as well as terminal and base stations positions. In order to calculate bounds on the localization error during NLoS propagation, not only must the locations of measuring base stations and mobile terminal be known but also the geometry of obstacles to radio

propagation. When the conditional distribution of measurements is not continuous, the 'regularity' conditions of the Cramér-Rao bound are not satisfied. NLoS propagation creates discontinuities in the derivatives of the conditional probability density functions of the measurements on the border of NLoS regions where the propagation switches from LoS to NLoS.

Prior work on the development of localization error bounds in the presence of both NLoS and LoS propagation has demonstrated that where some base stations have LoS propagation and the other base stations have NLoS propagation, only the measurements from LoS base stations need to be considered to calculate a valid Cramér-Rao lower bound (Qi and Kobayashi, 2002, Botteron et al., 2004). This work modeled NLoS propagation as a random effect with no correlation to a node's location. In this case, the occurrence of NLoS propagation only degrades localization accuracy. However, in practice, NLoS propagation at some locations is deterministic as the LoS propagation paths to measuring base stations are blocked by large immobile objects such as walls or buildings.

2. **The localizations are locally unbiased.** For a locally unbiased estimator, $\mathrm{E}[\hat{\boldsymbol{\theta}}(k) \mid \boldsymbol{\theta}(k)] = \boldsymbol{\theta}(k)$. Terminal localization made using ToA or TDoA measurements are rarely unbiased because of the non-linear relationship of the measurement vector with the terminal location (Kim et al. 2001). If an expression for the bias can be calculated, it is possible to calculate a modified form of (7) which takes bias into account (Kay, 1993). Unfortunately, analysis of zero memory estimators has shown that closed form expressions for this bias are extremely difficult, if not impossible, to obtain (Torrieri 1984). Such a closed form expression would be equivalent to a closed form solution to (3) which is non-trivial for any $f(\mathbf{z}(k) \mid \boldsymbol{\theta}(k))$ conditional probability density function of reasonable complexity. It is known, that for some geometries of base station and node locations, the bias can be quite large in proportion to the total estimation error (Torrieri 1984; Spirito 2001). An example of a base station geometry resulting in a large bias is when the base stations' locations are all collinear with the node location.

   This condition is separate from the condition that localization is globally unbiased, which is the condition that $\mathrm{E}[\hat{\boldsymbol{\theta}}(k)] = \mathrm{E}[\boldsymbol{\theta}(k)]$. Clearly, a locally unbiased estimator is also globally unbiased but the converse is not always true. For example, the trivial localization system that $\hat{\boldsymbol{\theta}}(k) = \mathrm{E}[\boldsymbol{\theta}(k)]$ for all $\mathbf{z}(k)$ is globally unbiased but is not locally unbiased.
3. **No information is available on the node location aside from the measurement vector.** This assumption is required for the Cramér-Rao bound to be a true lower bound. In an urban or indoor region, base stations are located throughout the network area. As a mobile terminal moves through the network area, the hand off algorithm ensures that the mobile terminal is always communicating with a base station that is close to its location. Furthermore, base stations close to the mobile terminal are more likely to be making measurements for localization than base stations further away from the mobile terminal. Therefore, the base station selection for localization is not independent of terminal location. These two factors indicate that the wireless sensor network has prior statistical knowledge of the terminal location before any measurements are made. This knowledge is, in fact, the basis of Phase I of the FCC's E911 wireless location requirement for cellular telephone localization, where the network can identify from which cell a user is making a cellular telephone call (Federal Communications Commission, 1996).

The two largest problems for the calculation of localization error bounds are the unknown bias in the location estimates, and the existence of information on mobile terminal position available prior to the localization. The next section will describe how lower bounds on localization error are calculated in this case.

LOWER BOUNDS ON LOCATION ESTIMATION ERROR WITH PRIOR INFORMATION

If information on the node location is available before the localization procedure begins, then a Bayesian localization procedure with localization MSE that is lower than the Cramér-Rao bound described above is available. To bound this estimator, a Bayesian lower bound on the localization error is required. The most common Bayesian bound is the Bayesian Cramér-Rao Bound (BCRB) given by

$$\mathrm{E}\{[\boldsymbol{\theta}(k)-\hat{\boldsymbol{\theta}}(k)][\boldsymbol{\theta}(k)-\hat{\boldsymbol{\theta}}(k)]^T\} \geq \{\tilde{\mathbf{J}}[\boldsymbol{\theta}(k)]\}^{-1} \tag{10}$$

where the matrix $\tilde{\mathbf{J}}[\boldsymbol{\theta}(k)]$ is defined as

$$\tilde{\mathbf{J}}[\boldsymbol{\theta}(k)] = -\mathrm{E}\{\nabla_{\boldsymbol{\theta}(k)}[\nabla_{\boldsymbol{\theta}(k)} \log f(\mathbf{z}(k),\boldsymbol{\theta}(k))]^T\} \tag{11}$$

when $f(\mathbf{z}(k),\boldsymbol{\theta}(k))$ is the joint probability density function of $\mathbf{z}(k)$ and $\theta(k)$ with no restrictions on the bias of the estimator for bound validity (Van Trees, 2001). The inequality of $\mathbf{A} \geq \mathbf{B}$ indicates that the matrix given by $\mathbf{D} = \mathbf{A} - \mathbf{B}$ is non-negative definite. Using standard Bayesian theory, the joint probability density function is given by $f(\mathbf{z}(k),\boldsymbol{\theta}(k)) = f(\mathbf{z}(k)\,|\,\boldsymbol{\theta}(k))f(\boldsymbol{\theta}(k))$ where $f(\mathbf{z}(k)\,|\,\boldsymbol{\theta}(k))$ is the conditional probability density function used to calculate the standard Cramér-Rao bound above. The probability density function $f(\boldsymbol{\theta}(k))$ represents the prior probability density function for the mobile terminal location given the selection of measuring base stations or other information.

A useful property of the BCRB is that the effects of the measurements and the prior information are easily separated in terms of computation. This separation is obtained by factoring the measurement conditional probability density function from the joint probability density function of the measurements and location:

$$\tilde{\mathbf{J}}[\boldsymbol{\theta}(k)] = \tilde{\mathbf{J}}_D[\boldsymbol{\theta}(k)] + \tilde{\mathbf{J}}_P[\boldsymbol{\theta}(k)] \tag{12}$$

where if $\mathrm{I}\{g[\boldsymbol{\theta}(k)]\} = -\mathrm{E}\{\nabla_{\boldsymbol{\theta}(k)}[\nabla_{\boldsymbol{\theta}(k)} \log \mathrm{g}(\boldsymbol{\theta}(k))]^T\}$ then $\tilde{\mathbf{J}}_D[\boldsymbol{\theta}(k)] = \mathrm{I}[f(\mathbf{z}(k)\,|\,\boldsymbol{\theta}(k))]$ and $\tilde{\mathbf{J}}_P[\boldsymbol{\theta}(k)] = \mathrm{I}[f(\boldsymbol{\theta}(k))]$. The information matrix $\tilde{\mathbf{J}}_D[\boldsymbol{\theta}(k)]$ is the statistical expectation of the standard Cramér-Rao bound over all possible node locations and quantifies the information from the measurement vector on the localization error bound and the information matrix $\tilde{\mathbf{J}}_P[\boldsymbol{\theta}(k)]$ quantifies the effect of the prior information on the localization error bound. For stationary nodes, the source of the prior information represents information from the selection of base stations used for localization. When non-stationary nodes are located, this prior information can also represent information from measurements in previous sample intervals. More information on this latter case is provided in a later section of this chapter. The computation of the BCRB for localization error using Monte Carlo integration is summarized as Algorithm 1. This calculation gives better approximations to the true bound as $N \to \infty$.

Unfortunately, the BCRB does not exist for all estimation problems. For the BCRB to be valid, two conditions are required (Van Trees 2001). The first condition is that the first and second order partial derivatives of $f(\mathbf{z}(k),\boldsymbol{\theta}(k))$ with respect to all entries of $\theta(k)$ must be absolutely integrable with respect to the entries of $\mathbf{z}(k)$ and $\boldsymbol{\theta}(k)$. The second condition is that the matrices $\tilde{\mathbf{J}}_D[\boldsymbol{\theta}(k)]$ and $\tilde{\mathbf{J}}_P[\boldsymbol{\theta}(k)]$ must be invertible.

The existence of NLoS propagation creates discontinuities in the first and second partial derivatives of $f(\mathbf{z}(k),\boldsymbol{\theta}(k))$ with respect to the entries of $\boldsymbol{\theta}(k)$. The discontinuities occur at the boundaries between regions of LoS and NLoS propagation creating impulses in the partial derivatives of the joint probability density function. The second order partial derivatives in (11) become unbounded, which makes the BCRB invalid. In addition, if the second partial derivatives of $f(\boldsymbol{\theta}(k))$ with respect to the entries of $\boldsymbol{\theta}(k)$ are unbounded then the BCRB is invalidated. This condition is created for many common prior density functions. For example, if the node location is uniformly distributed over a finite area, the second partial derivatives of $f(\boldsymbol{\theta}(k))$ are infinite at the boundaries of the region of support for $f(\boldsymbol{\theta}(k))$ invalidating the BCRB.

The BCRB provides a perfect calculation of the optimal MSE when the conditional probability density function $f\left(\boldsymbol{\theta}(k)\,|\,\mathbf{z}(k)\right)$ is a multivariate Gaussian probability density function for all $\mathbf{z}(k)$ (Van Trees 2001). The non-linearity of the relationship between the measurements and terminals locations means that this is rarely the case for the localization problem. However, the BCRB provides MSE bounds close to the actual optimal MSE when $f\left(\boldsymbol{\theta}(k)\,|\,\mathbf{z}(k)\right)$ is well approximated by a multivariate Gaussian probability density function in that there exists a multivariate Gaussian probability density function, $f_G(\boldsymbol{\theta}(k))$ such that for some small constant ε, $\left|f(\boldsymbol{\theta}(k)\,|\,\mathbf{z}(k)) - f_G(\boldsymbol{\theta}(k))\right| < \varepsilon$ for all $\boldsymbol{\theta}(k)$ and $\mathbf{z}(k)$. When this is not true, then the BCRB MSE bound value can be significantly lower than the true MSE.

Because of these problems, other bounds are needed to calculate a bound on the MSE for localization in the presence of NLOS propagation. The discontinuities created by the presence of both LOS and NLOS propagation in the mobile terminal environment can be handled by either the Barankin bound, the Weinstein-Weiss bound or the extended Ziv-Zakai bound, as can be seen in Table 1. The Barankin bound is valid for localization MSE if the mobile terminal location is deterministic. If there exists a prior probability density function for $\theta(k)$, then the Weinstein-Weiss or extended Ziv-Zakai lower bounds are applicable.

Algorithm 1. Monte Carlo integration calculation of Bayesian Cramér-Rao bound

1. Generate N independent samples of $\boldsymbol{\theta}(k)$: $\mathbf{t}^1$, $\mathbf{t}^2$, …, $\mathbf{t}^N$
   $\mathbf{t}^k$ has probability density function of $f(\boldsymbol{\theta}(k))$
2. Calculate $\tilde{\mathbf{J}}_D(\boldsymbol{\theta}(k))$:
   $$\tilde{\mathbf{J}}_D(\boldsymbol{\theta}(k)) = \frac{1}{N}\sum_{k=1}^{N}(\mathbf{D}^k)^T\mathbf{C}^{-1}(\mathbf{D}^k) \text{ where } \mathbf{D}^k = \nabla_{\boldsymbol{\theta}(k)} \mathrm{E}[\mathbf{z}(k)\,|\,\boldsymbol{\theta}(k)]\Big|_{\boldsymbol{\theta}(k)=\mathbf{t}^k}$$
3. Calculate $\tilde{\mathbf{J}}_P(\boldsymbol{\theta}(k))$:
   $$\tilde{\mathbf{J}}_P(\boldsymbol{\theta}(_k)) = -\frac{1}{N}\sum_{k=1}^{N}\mathbf{B}^k \text{ where } \mathbf{B}^k = \nabla_{\boldsymbol{\theta}(k)}\left[\nabla_{\boldsymbol{\theta}(k)} \log{}_f(\boldsymbol{\theta}(k))\right]^T\Big|_{\boldsymbol{\theta}(k)=\mathbf{t}^k}$$
4. Calculate bound on localization MSE from (10).

The Weinstein-Weiss Lower Bound

The Weinstein-Weiss lower bound gives a lower bound on the MSE of any estimator (Weinstein and Weiss, 1988). The basis of the Weinstein-Weiss bound is that for any vector function e($\mathbf{z}(k)$), the following inequality holds:

$$\mathrm{E}\{[\boldsymbol{\theta}(k)-\mathrm{e}(\mathbf{z}(k))][\boldsymbol{\theta}(k)-\mathrm{e}(\mathbf{z}(k))]^{T}\} \geq \mathbf{H}\mathbf{G}^{-1}\mathbf{H}^{\mathrm{T}} \tag{13}$$

where $\mathbf{G}$ is the matrix with entries given by

$$\mathbf{G}_{i,j} = \frac{\mathrm{E}\{\mathrm{M}[\mathrm{s}_i,\mathbf{z}(k),\mathbf{h}_i]\mathrm{M}[\mathrm{s}_j,\mathbf{z}(k),\mathbf{h}_i]\}}{\mathrm{E}\{\mathrm{L}^{s_i}[\mathbf{z}(k),\boldsymbol{\theta}(k)+\mathbf{h}_i,\boldsymbol{\theta}(k)]\}\,\mathrm{E}\{\mathrm{L}^{s_j}[\mathbf{z}(k),\boldsymbol{\theta}(k)+\mathbf{h}_j,\boldsymbol{\theta}(k)]\}} \tag{14}$$

with $\mathbf{H}=[\mathbf{h}_1\mathbf{h}_2]$ for any vectors ($\mathbf{h}_1$,$\mathbf{h}_2$) and scalars (s_1,s_2). The functions $\mathrm{L}^{\mathrm{s}}[\mathbf{z}(k),\boldsymbol{\theta}(k)+\mathbf{h},\boldsymbol{\theta}(k)]$ are defined as

$$\mathrm{L}^{\mathrm{s}}[\mathbf{z}(k),\boldsymbol{\theta}(k)+\mathbf{h},\boldsymbol{\theta}(k)] = \left[\frac{f(\mathbf{z}(k),\boldsymbol{\theta}(k)+\mathbf{h})}{f(\mathbf{z}(k),\boldsymbol{\theta}(k))}\right]^{s}, \tag{15}$$

and the function $\mathrm{M}[\mathrm{s},\mathbf{z}(k),\boldsymbol{\theta}(k),\mathbf{h}]$ is defined as

$$\mathrm{M}[\mathrm{s},\mathbf{z}(k),\boldsymbol{\theta}(k),\mathbf{h}] = \mathrm{L}^{\mathrm{s}}[\mathbf{z}(k),\boldsymbol{\theta}(k)+\mathbf{h},\boldsymbol{\theta}(k)] - \mathrm{L}^{1-\mathrm{s}}[\mathbf{z}(k),\boldsymbol{\theta}(k)-\mathbf{h},\boldsymbol{\theta}(k)]. \tag{16}$$

All expectations are taken with respect to $f(\mathbf{z}(k),\boldsymbol{\theta}(k))$; that is, with regards to both the measurements and the mobile terminal location. Since for any localization system $\hat{\boldsymbol{\theta}}(k)=\mathrm{e}(\mathbf{z}(k))$, the bound in (13) is also a bound on the MSE of any localization system. The tightest Weinstein-Weiss lower bound is achieved by calculating the values of s_1, s_2, $\mathbf{h}_1$, and $\mathbf{h}_2$ that maximize the right hand side of (13). Finding the tightest bound is a computationally expensive task.

Fortunately, any set of values of s_1, s_2, $\mathbf{h}_1$, and $\mathbf{h}_2$ bound the estimator performance. Selecting $s_1 = s_2 = 1/2$ and

$$\mathbf{H} = h\begin{bmatrix} 1 & 0 \\ 0 & 1 \end{bmatrix} \tag{17}$$

results in a bound with a very practical cost. For these values, the elements of $\mathbf{G}$ can be rewritten as

$$\mathbf{G}_{i,j} = 2\frac{\mu\left(\frac{1}{2},\mathbf{h}_i-\mathbf{h}_j\right)-\mu\left(\frac{1}{2},\mathbf{h}_i+\mathbf{h}_j\right)}{\mu\left(\frac{1}{2},\mathbf{h}_i\right)\mu\left(\frac{1}{2},\mathbf{h}_j\right)} \tag{18}$$

with $\mu(s,\mathbf{h}) = \mathrm{E}\{\mathrm{L}^{s}[\mathbf{z}(k),\boldsymbol{\theta}(k)+\mathbf{h},\boldsymbol{\theta}(k)]\}$ where $\mathbf{h}_i$ and $\mathbf{h}_j$ designate the i^{th} and j^{th} respective columns of the matrix $\mathbf{H}$. A tight bound can be found by finding the value h which maximizes (13) with the other variables set as above. The limit of this case for $h \rightarrow 0$ results in the BCRB, provided the BCRB's conditions are satisfied. As stated above, the BCRB conditions are rarely satisfied in the wireless terminal localization application, but this shows that the best Weinstein-Weiss bound will be at least as tight to optimal localization performance as the BCRB in cases where both bounds are valid.

The special case of $\mu(1/2,\mathbf{h})$ is simplified as

$$\begin{aligned}
\mu\left(\frac{1}{2},\mathbf{h}\right) &= \mathrm{E}\left\{\left[\frac{f(\mathbf{z}(k),\boldsymbol{\theta}(k)+\mathbf{h})}{f(\mathbf{z}(k),\boldsymbol{\theta}(k))}\right]^{\frac{1}{2}}\right\} \qquad (19)\\
&= \int_{\mathbf{S}(k)}\int_{\Re^{l}}\left[\frac{f(\mathbf{z}(k),\boldsymbol{\theta}(k)+\mathbf{h})}{f(\mathbf{z}(k),\boldsymbol{\theta}(k))}\right]^{\frac{1}{2}} f(\mathbf{z}(k),\boldsymbol{\theta}(k))\mathrm{d}\mathbf{z}(k)\mathrm{d}\boldsymbol{\theta}(k)\\
&= \int_{\mathbf{S}(k)}\int_{\Re^{l}}\left[f(\mathbf{z}(k),\boldsymbol{\theta}(k)+\mathbf{h})\right]^{\frac{1}{2}}\left[f(\mathbf{z}(k),\boldsymbol{\theta}(k))\right]^{\frac{1}{2}}\mathrm{d}\mathbf{z}(k)\mathrm{d}\boldsymbol{\theta}(k)\\
&= \int_{\mathbf{S}(k)}\int_{\Re^{l}}\left[f(\mathbf{z}(k)\,|\,\boldsymbol{\theta}(k)+\mathbf{h})f(\boldsymbol{\theta}(k)+\mathbf{h})\right]^{\frac{1}{2}}\left[f(\mathbf{z}(k)\,|\,\boldsymbol{\theta}(k))f(\boldsymbol{\theta}(k))\right]^{\frac{1}{2}}\mathrm{d}\mathbf{z}(k)\mathrm{d}\boldsymbol{\theta}(k)
\end{aligned}$$

where $f(\boldsymbol{\theta}(k))$ is the prior probability density function for the node location with support $\mathbf{S}$(k), and the measurement vectors are of length l. If the measurement vectors given the node locations are Gaussian the conditional probability density function of the measurement vector $\mathbf{z}(k)$ given the location $\boldsymbol{\theta}(k)$ is

$$f(\mathbf{z}(k)\,|\,\boldsymbol{\theta}(k)) = (2\pi)^{-l/2}\left|\mathbf{C}\right|^{-1/2}\exp\left(-\frac{1}{2}\left\|\tilde{\mathbf{z}}[\boldsymbol{\theta}(k)]\right\|_{\mathbf{C}^{-1}}^{2}\right) \qquad (20)$$

with the signal difference vector defined as $\tilde{\mathbf{z}}[\boldsymbol{\theta}(k)] = \mathbf{z}(k) - \mathrm{E}[\mathbf{z}(k)\,|\,\boldsymbol{\theta}(k)]$ where $\mathrm{E}[\mathbf{z}(k)\,|\,\boldsymbol{\theta}(k)]$ is the expected measurement vector given the wireless node is at position $\boldsymbol{\theta}(k)$, and $\mathbf{C}$ is the covariance matrix of the measurement vector given the node position $\boldsymbol{\theta}(k)$. To simplify the expressions for the Gaussian probability density functions, we make use of the Mahalanobis quadratic distance function defined as $\left\|\mathbf{x}\right\|_{\mathbf{C}^{-1}}^{2} = \mathbf{x}^{T}\mathbf{C}^{-1}\mathbf{x}$ (Duda et al. 01). Substituting (20) into (19), the $\mu(1/2,\mathbf{h})$ is defined as

$$\begin{aligned}
\mu\left(\frac{1}{2},\mathbf{h}\right) = \int_{\mathbf{S}(k)}\int_{\Re^{l}}(2\pi)^{-\frac{l}{2}}\left|\mathbf{C}\right|^{-\frac{1}{2}}\exp\left\{-\frac{1}{4}\left[\left\|\tilde{\mathbf{z}}[\boldsymbol{\theta}(k)]\right\|_{\mathbf{C}^{-1}}^{2} + \left\|\tilde{\mathbf{z}}[\boldsymbol{\theta}(k)+\mathbf{h}]\right\|_{\mathbf{C}^{-1}}^{2}\right]\right\}\\
\times[f(\boldsymbol{\theta}(k))f(\boldsymbol{\theta}(k)+\mathbf{h})]^{\frac{1}{2}}\mathrm{d}\mathbf{z}(k)\mathrm{d}\boldsymbol{\theta}(k) \qquad (21)
\end{aligned}$$

To simplify (21), we expand the Gaussian density functions, complete the squares, and then integrate to obtain

$$\mu\left(\frac{1}{2},\mathbf{h}\right)=\int\limits_{\mathbf{S}(k)}\exp\left\{-\frac{1}{8}\left\|\mathrm{E}[\mathbf{z}(k)\,|\,\boldsymbol{\theta}(k)]-\mathrm{E}[\mathbf{z}(k)\,|\,\boldsymbol{\theta}(k)+\mathbf{h}]\right\|_{\mathbf{C}^{-1}}^{2}\right\}[f(\boldsymbol{\theta}(k))f(\boldsymbol{\theta}(k)+\mathbf{h})]^{\frac{1}{2}}\,\mathrm{d}\boldsymbol{\theta}(k). \tag{22}$$

In general, except for very simple node arrangements, (22) can only be integrated numerically.

For the two dimensional localization problem, the matrix **G** from (18) is given by

$$\mathbf{G}=2\begin{bmatrix}\dfrac{\mu\left(\frac{1}{2},\begin{bmatrix}0\\0\end{bmatrix}\right)-\mu\left(\frac{1}{2},\begin{bmatrix}2h\\0\end{bmatrix}\right)}{\mu\left(\frac{1}{2},\begin{bmatrix}h\\0\end{bmatrix}\right)^{2}} & \dfrac{\mu\left(\frac{1}{2},\begin{bmatrix}h\\-h\end{bmatrix}\right)-\mu\left(\frac{1}{2},\begin{bmatrix}h\\h\end{bmatrix}\right)}{\mu\left(\frac{1}{2},\begin{bmatrix}h\\0\end{bmatrix}\right)\mu\left(\frac{1}{2},\begin{bmatrix}0\\h\end{bmatrix}\right)}\\[2ex] \dfrac{\mu\left(\frac{1}{2},\begin{bmatrix}-h\\h\end{bmatrix}\right)-\mu\left(\frac{1}{2},\begin{bmatrix}h\\h\end{bmatrix}\right)}{\mu\left(\frac{1}{2},\begin{bmatrix}h\\0\end{bmatrix}\right)\mu\left(\frac{1}{2},\begin{bmatrix}0\\h\end{bmatrix}\right)} & \dfrac{\mu\left(\frac{1}{2},\begin{bmatrix}0\\0\end{bmatrix}\right)-\mu\left(\frac{1}{2},\begin{bmatrix}0\\2h\end{bmatrix}\right)}{\mu\left(\frac{1}{2},\begin{bmatrix}0\\h\end{bmatrix}\right)^{2}}\end{bmatrix}. \tag{23}$$

The matrix **G** from (23) is then substituted into (13) to obtain the final Weinstein-Weiss bound matrix. From this matrix, it is possible to calculate a lower bound on the MSE for the localization of stationary nodes. The calculation of the Weinstein-Weiss lower bound for localization using Monte Carlo integration is summarized in Algorithm 2.

The Weinstein-Weiss bound's primary advantage compared to the BCRB is that it handles a wider variety of measurement conditional and location prior probability density functions. It provides MSE bounds close to the optimal MSE values when the conditional probability density function $f(\boldsymbol{\theta}(k)\,|\,\mathbf{z}(k))$ is well approximated as a multivariate Gaussian probability density function (Van Trees and Bell 2007). When this approximation is not good, the Weinstein-Weiss bound is significantly less than the optimal MSE. This is similar to the BCRB, but the Weinstein-Weiss bound is still valid when the prior probability density function $f(\boldsymbol{\theta}(k))$ has only finite support while the BCRB becomes invalid in this case.

While the Weinstein-Weiss lower bound works well in most cases, there are some cases where it can be difficult to calculate, such as when a closed form for $f(\mathbf{z}(k),\boldsymbol{\theta}(k))$ is not available or it is difficult to integrate. In these cases, the Extended Ziv-Zakai bound may be easier to compute.

Algorithm 2: Monte Carlo Integration of Weinstein Weiss bound

The Extended Ziv-Zakai Lower Bound for Location

The Extended Ziv-Zakai lower bound provides a lower bound on the estimation error for Bayesian estimation based on binary detection theory (Bell et al. 1997). The calculation provides a lower bound on the value of $\mathbf{a}^T\mathbf{R}_\mathbf{e}\mathbf{a}$, where $\mathbf{R}_\mathbf{e}=\mathrm{E}\{[\boldsymbol{\theta}(k)-\hat{\boldsymbol{\theta}}(k)][\boldsymbol{\theta}(k)-\hat{\boldsymbol{\theta}}(k)]^T\}$. By suitable selections of the vector **a**, bounds can be calculated for all entries of the matrix $\mathbf{R}_\mathbf{e}$.

The bound is based on the binary detection problem of deciding whether a mobile terminal is located at position θ(*k*) or at position $\boldsymbol{\theta}(k)+\boldsymbol{\delta}$ given the measurement vector **z**(*k*). If the greatest lower bound

Algorithm 2. Monte Carlo Integration of Weinstein Weiss bound

1. Compute Weinstein-Weiss bound for a sweep of h values.
   a. Set **H** according to (17) for selected h value.
   b. Compute $\mu(1/2,\bullet)$ function values for entries of **G** from (23) using sub-algorithm below.
   c. Compute bound from **G** and **H** using (13)
2. For the MSE bounds with different h values calculated in step 1, select the highest MSE as the Weinstein-Weiss bound.

   Sub-algorithm: Calculation of $\mu(1/2,\mathbf{h})$

   a) Generate N independent samples of $\boldsymbol{\theta}(k)$: $\mathbf{t}^1, \mathbf{t}^2, \ldots, \mathbf{t}^N$

   $\mathbf{t}^k$ has the probability density function $f(\boldsymbol{\theta}(k))$

   b) Compute:

   $$\mathbf{c}_k = \exp\left\{-\frac{1}{8}\left\|\mathrm{E}[\mathbf{z}(k)\,|\,\boldsymbol{\theta}(k)=\mathbf{t}^k] - \mathrm{E}[\mathbf{z}(k)\,|\,\boldsymbol{\theta}(k)=\mathbf{t}^k+\mathbf{h}]\right\|^2_{\mathbf{C}^{-1}}\left[f(\boldsymbol{\theta}(k)=\mathbf{t}^k)f(\boldsymbol{\theta}(k)=\mathbf{t}^k+\mathbf{h})\right]^{\frac{1}{2}}\right\}$$

   c) Compute $\mu(1/2,\mathbf{h}) = \frac{1}{N}\sum_{k=1}^{N}\mathbf{c}_k$

on the probability on this decision error is given by $\mathrm{P}_{\min}[\boldsymbol{\theta}(k),\boldsymbol{\theta}(k)+\boldsymbol{\delta}]$, then the extended Ziv-Zakai bound is written as

$$\mathbf{a}^T\mathbf{R}_{\mathbf{e}}\mathbf{a} \geq \frac{1}{2}\int_0^\infty h\,\mathrm{V}\left\{\max_{\boldsymbol{\delta}:\mathbf{a}^T\boldsymbol{\delta}=\mathbf{h}}\left[\int_{\mathbf{S}(k)}[f(\boldsymbol{\theta}(k))+f(\boldsymbol{\theta}(k)+\boldsymbol{\delta})]\,\mathrm{P}_{\min}[\boldsymbol{\theta}(k),\boldsymbol{\theta}(k)+\boldsymbol{\delta}]\mathrm{d}\boldsymbol{\theta}(k)\right]\right\}\mathrm{d}h\,. \qquad (24)$$

The $\mathrm{V}[g(h)]$ is the so-called valley-filling function defined as $\mathrm{V}\left[\mathrm{g}(h)\right] = \max_{x\geq h}\mathrm{g}(x)$. The tightest bound is found by performing the maximization to find the best value of δ for each value of h. However, the use of any vector δ subject to $\mathbf{a}^T\boldsymbol{\delta} = h$ still results in valid bound, available at a reduced computational cost.

Standard Bayesian detection theory is used to calculate the greatest lower bound on the decision error (Van Trees 2001). If the prior $f(\boldsymbol{\theta}(k))$ is uniform over a finite region and the measurement vector $\mathbf{z}(k)$ given the node location $\boldsymbol{\theta}(k)$ is a Gaussian random vector with mean $\mathrm{E}[\mathbf{z}(k)\,|\,\boldsymbol{\theta}(k)]$ and a covariance matrix of $\mathbf{C} = \mathbf{I}^m\sigma^2$ for all locations then the minimum error probability is

$$\mathrm{P}_{\min}[\boldsymbol{\theta}(k),\boldsymbol{\theta}(k)+\boldsymbol{\delta}] = \mathrm{P}^{el}_{\min}[\boldsymbol{\theta}(k),\boldsymbol{\theta}(k)+\boldsymbol{\delta}] = \mathrm{erfc}\left(\frac{\left\|\mathrm{E}[\mathbf{z}(k)\,|\,\boldsymbol{\theta}(k)] - \mathrm{E}[\mathbf{z}(k)\,|\,\boldsymbol{\theta}(k)+\boldsymbol{\delta}]\right\|}{2\sqrt{2}\sigma}\right) \qquad (25)$$

with $\|\mathbf{v}\|$ being the Euclidean length of vector $\mathbf{v}$ (Van Trees 2001). Substituting (25) into (24), and then using a numerical integration technique, such as Monte Carlo integration, provides a general method for bounding localization MSE.

For a general prior probability density functions, the lower bound of (24) can be difficult to compute. In these cases, a looser lower bound is obtained at a much lower cost from the computation of

$$\mathbf{a}^T\mathbf{R}_{\mathbf{e}}\mathbf{a} \geq \int_0^\infty h\,\mathrm{V}\left\{\max_{\boldsymbol{\delta}:\mathbf{a}^T\boldsymbol{\delta}=h}\left[\int_{\mathbf{S}(k)}\min[f(\boldsymbol{\theta}(k)),f(\boldsymbol{\theta}(k)+\boldsymbol{\delta})]\,\mathrm{P}^{el}_{\min}[\boldsymbol{\theta}(k),\boldsymbol{\theta}(k)+\boldsymbol{\delta}]\mathrm{d}\boldsymbol{\theta}(k)\right]\right\}\mathrm{d}h \qquad (26)$$

where $P^{el}_{\min}[\boldsymbol{\theta}(k),\boldsymbol{\theta}(k)+\boldsymbol{\delta}]$ is the optimum decision error between θ(*k*) and $\boldsymbol{\theta}(k)+\boldsymbol{\delta}$ calculated using the assumption that both locations are equally likely, so $P^{el}_{\min}[\boldsymbol{\theta}(k),\boldsymbol{\theta}(k)+\boldsymbol{\delta}] = P_{\min}[\boldsymbol{\theta}(k),\boldsymbol{\theta}(k)+\boldsymbol{\delta}]$ with $P_{\min}[\boldsymbol{\theta}(k),\boldsymbol{\theta}(k)+\boldsymbol{\delta}]$ from (25) (Bell et al., 1997). The extended Ziv-Zakai bound calculation using Monte Carlo integration is summarized in Algorithm 3.

Bounds for Location Accuracy from Survey Set Information

For complex propagation environments, such as those encountered in indoor or dense urban locations, simple analytical propagation models, such as those described in the second section of this chapter, do not adequately describe the measurement model to determine the terminal localization accuracy. In these cases, the main recourse for the network designer is to collect survey points in the environment for the implementation of node localization. This section shows a simple calculation that allows a network designer to solve for MSE bounds on the accuracy of localization in their network using a propagation survey set collected in the network area. This calculation is based upon the extended Ziv-Zakai bound presented in the previous section with some modifications for the discrete nature of the survey set information.

Two assumptions are made about the survey set for this procedure to be valid. It is first assumed that the survey set measurements are noise free, in that the survey measurement for a given location is the expected measurement for that location. It is also assumed that the survey set locations are dense enough in the network environment to provide a good representation of the expected variation of the signal measurements over the network area. In other words, these two assumptions state that it is possible to reconstruct all major features of the mean signal function $E[\mathbf{z}(k)\,|\,\boldsymbol{\theta}(k)]$ from some interpolation of the survey set. Both of these assumptions are standard requirements for the construction of good localization systems based on survey data so are not additional requirements over those of standard survey-based radio localization (McGuire et al., 2003a).

This bounding procedure assumes that the measurement noise distribution is identical for all locations. This assumption is well met if a sensor selection system is used to ensure that only sensors with

Algorithm 3. Calculation of extended Ziv-Zakai bound

1. Numerically integrate $\int_0^\infty h\,\mathrm{V}\left[g(h)\right]dh$ for lower bound on $\mathbf{a}^T\mathbf{R}_e\mathbf{a}$ for $\mathbf{a}$=[1 0]^T
   a. $g(h) = \nu(\boldsymbol{\delta})$ where $\boldsymbol{\delta}$ is selected to maximize $\nu(\boldsymbol{\delta})$ subject to $\mathbf{a}^T\boldsymbol{\delta} = h$
      i. Option: for a quick but looser bound, select $\boldsymbol{\delta} = h\mathbf{a}$ where $|\mathbf{a}| = 1$
2. Numerically integrate $\int_0^\infty h\,\mathrm{V}\left[g(h)\right]dh$ for lower bound on $\mathbf{a}^T\mathbf{R}_e\mathbf{a}$ for $\mathbf{a}$=[0 1]^T
3. Combine results from step 1 and 2 to obtain extended Ziv-Zakai bound.

Sub-algorithm: Calculation of $\nu(\boldsymbol{\delta})$

a) Generate N independent samples of $\boldsymbol{\theta}(k)$: $\mathbf{t}^1, \mathbf{t}^2, \ldots, \mathbf{t}^N$
b) Compute:
$$\mathbf{c}_k = \min[f(\boldsymbol{\theta}(k)=\mathbf{t}^k), f(\boldsymbol{\theta}(k)=\mathbf{t}^k+\boldsymbol{\delta})]\,P^{el}_{\min}(\boldsymbol{\theta}(k)=\mathbf{t}^k, \boldsymbol{\theta}(k)+\boldsymbol{\delta}=\mathbf{t}^k+\boldsymbol{\delta})$$
where $P^{el}_{\min}(\boldsymbol{\theta}(k)=\mathbf{t}^k, \boldsymbol{\theta}(k)+\boldsymbol{\delta}=\mathbf{t}^k+\boldsymbol{\delta})$ is computed using (25).
c) Compute $\nu(\boldsymbol{\delta}) = \frac{1}{N}\sum_{k=1}^{N}\mathbf{c}_k$

high signal-to-noise ratios (SNRs) are used for the localization procedure. Since using other sensors will contribute little to the accuracy of the system and incur a communications cost penalty, this restriction will be satisfied by most real world localization systems.

By defining the non-negative random variable $\varepsilon = |\hat{\boldsymbol{\theta}}(k) - \boldsymbol{\theta}(k)|$, the MSE of the estimation error is computed with the expression

$$\mathrm{E}[\varepsilon^2] = \frac{1}{2}\int_0^\infty \Pr\left(\varepsilon \geq \frac{h}{2}\right) h \mathrm{d}h. \tag{27}$$

To use the survey points to compute a bound on the MSE, it is assumed that the survey points represent all possible locations for the nodes, and that all survey point locations are equally likely. This is equivalent to the expression that

$$\Pr(\boldsymbol{\theta}(k) = \tilde{\boldsymbol{\theta}}^i) = 1/N \tag{28}$$

with $\tilde{\boldsymbol{\theta}}^i$ being the location of the i^{th} survey point and N being the total number of survey points. The probability of the error distance is bounded given the node location, assuming the measurement noise distribution is identical for all $\theta(k)$, as

$$\Pr[\varepsilon \geq e \mid \boldsymbol{\theta}(k) = \tilde{\boldsymbol{\theta}}^i] \geq \max_{j:\left\|\tilde{\boldsymbol{\theta}}^i - \tilde{\boldsymbol{\theta}}^j\right\| \geq e} \Pr\left(\left\|\mathbf{z}(k) - \tilde{\mathbf{z}}^j\right\| \leq \left\|\mathbf{z}(k) - \tilde{\mathbf{z}}^i\right\| \,\middle|\, \boldsymbol{\theta}(k) = \tilde{\boldsymbol{\theta}}^i\right) \tag{29}$$

where $\tilde{\mathbf{z}}^i$ and $\tilde{\mathbf{z}}^j$ being the measured signals for survey points i and j, respectively. Combining (28) with (29), the following probability bound is created:

$$\Pr\left(\varepsilon \geq e\right) \geq \frac{1}{N}\sum_{i=1}^{N} \max_{j:\left\|\tilde{\boldsymbol{\theta}}^i - \tilde{\boldsymbol{\theta}}^j\right\| \geq e} \Pr\left(\left\|\mathbf{z}(k) - \tilde{\mathbf{z}}^j\right\| \leq \left\|\mathbf{z}(k) - \tilde{\mathbf{z}}^i\right\| \,\middle|\, \boldsymbol{\theta}(k) = \tilde{\boldsymbol{\theta}}^i\right). \tag{30}$$

To obtain the final bound, equation (30) is substituted into (27) to obtain

$$\mathrm{E}\left[\varepsilon^2\right] \geq \frac{1}{2}\int_0^\infty h \frac{1}{N}\sum_{i=1}^{N} \max_{j:\left\|\tilde{\boldsymbol{\theta}}^i - \tilde{\boldsymbol{\theta}}^j\right\| \geq \frac{h}{2}} \Pr\left(\left\|\mathbf{z}(k) - \tilde{\mathbf{z}}^j\right\| \leq \left\|\mathbf{z}(k) - \tilde{\mathbf{z}}^i\right\| \,\middle|\, \boldsymbol{\theta}\left(k\right) = \tilde{\boldsymbol{\theta}}^i\right) \mathrm{d}h\,. \tag{31}$$

For the simplifying assumption of the Gaussian measurement noise of (20) with $\mathbf{C} = \mathbf{I}^m \sigma^2$ then the probability from (30) is given by

$$\Pr\left(\left\|\mathbf{z}(k) - \tilde{\mathbf{z}}^j\right\| \leq \left\|\mathbf{z}(k) - \tilde{\mathbf{z}}^i\right\| \,\middle|\, \boldsymbol{\theta}\left(k\right) = \tilde{\boldsymbol{\theta}}^i\right) = \frac{1}{2}\mathrm{erfc}\left(\frac{\left\|\tilde{\mathbf{z}}^i - \tilde{\mathbf{z}}^j\right\|}{2\sqrt{2\sigma^2}}\right). \tag{32}$$

To bound localization error using a survey set, the value of the noise covariance σ^2 is determined from measurements taken at a single location and then by substituting the survey set point locations and measurements into (31) using the probability from (32), a lower bound on the localization MSE is calculated.

To calculate the covariance bound, a discrete version of (24) is derived to obtain

$$\mathbf{a}^T \mathbf{R}_e \mathbf{a} \geq \frac{1}{2}\int_0^\infty h \frac{1}{N}\sum_{i=1}^{N} \max_{j:\left\|\mathbf{a}^T\left(\tilde{\boldsymbol{\theta}}^j - \tilde{\boldsymbol{\theta}}^i\right)\right\| \geq \frac{h}{2}} \Pr\left(\left\|\mathbf{z}(k) - \tilde{\mathbf{z}}^j\right\| \leq \left\|\mathbf{z}(k) - \tilde{\mathbf{z}}^i\right\| \,\middle|\, \boldsymbol{\theta}(k) = \tilde{\boldsymbol{\theta}}^i\right) \mathrm{d}h \,. \tag{33}$$

From (33) it is possible, with suitable selections of **a**, to calculate bounds on all entries of the squared error matrix, $\mathbf{R_e}$.

Bounds on Location for Multiple Measurements

The previous sections provide bounds on the localization accuracy from a single measurement vector. To consider additional measurements on the localization error bound, the obvious approach is to just extend the measurement vector, **z**(*k*), to include the new measurements. However, an easier approach is available if the measurement error for the new measurements, **z'**(*k*), is independent of the old measurement vector, **z**(*k*); i.e. $f(\mathbf{z}(k), \mathbf{z}'(k) \,|\, \boldsymbol{\theta}(k)) = f(\mathbf{z}(k) \,|\, \boldsymbol{\theta}(k)) f(\mathbf{z}'(k) \,|\, \boldsymbol{\theta}(k))$. In this case, the joint density of the measurements and location are

$$f(\mathbf{z}'(k), \mathbf{z}(k), \boldsymbol{\theta}(k)) = f(\mathbf{z}'(k) \,|\, \boldsymbol{\theta}(k)) f(\mathbf{z}(k) \,|\, \boldsymbol{\theta}(k)) f(\boldsymbol{\theta}(k)) = f(\mathbf{z}'(k) \,|\, \boldsymbol{\theta}(k)) f(\mathbf{z}(k), \boldsymbol{\theta}(k)) \tag{34}$$

so that we can consider the distribution of the location given both measurements as

$$f(\boldsymbol{\theta}(k) \,|\, \mathbf{z}(k), \mathbf{z}'(k)) = \frac{f(\mathbf{z}'(k) \,|\, \boldsymbol{\theta}(k)) f(\boldsymbol{\theta}(k) \,|\, \mathbf{z}(k))}{f(\mathbf{z}'(k) \,|\, \mathbf{z}(k))} \text{ with } f(\boldsymbol{\theta}(k) \,|\, \mathbf{z}(k)) = \frac{f(\boldsymbol{\theta}(k), \mathbf{z}(k))}{f(\mathbf{z}(k))}. \tag{35}$$

The denominators of the ratios in (35) are normalization constants and do not affect the localization. From (35), it can be seen that the conditional probability density function of **θ**(*k*) given **z**(*k*) and **z'**(*k*) is a normalized product of the conditional probability density functions of $f(\boldsymbol{\theta}(k) \,|\, \mathbf{z}(k))$ and $f(\mathbf{z}'(k) \,|\, \boldsymbol{\theta}(k))$. This motivates the use of a sequential estimation system where the prior probability density function $f(\boldsymbol{\theta}(k) \,|\, \mathbf{z}(k))$ is first calculated and then **θ**(*k*) is estimated from **z'**(*k*) using the prior distribution of $f(\boldsymbol{\theta}(k) \,|\, \mathbf{z}(k))$. This is the basis of the Kalman filter and all other sequential estimation algorithms (Mendel, 1995).

For bound computations using the BCRB considering additional measurements, the decomposition in (12) is extended using partial derivatives of the logarithm of (35) creating the BCRB matrix:

$$\tilde{\mathbf{J}}(\boldsymbol{\theta}(k)) = \tilde{\mathbf{J}}'_D(\boldsymbol{\theta}(k)) + \tilde{\mathbf{J}}_D(\boldsymbol{\theta}(k)) + \tilde{\mathbf{J}}_P(\boldsymbol{\theta}(k)) \tag{36}$$

with the information matrices $\tilde{\mathbf{J}}'_D(\boldsymbol{\theta}(k)) = \mathrm{I}[f(\mathbf{z}'(k) \,|\, \boldsymbol{\theta}(k))]$, $\tilde{\mathbf{J}}_D(\boldsymbol{\theta}(k)) = \mathrm{I}[f(\mathbf{z}(k) \,|\, \boldsymbol{\theta}(k))]$, and $\tilde{\mathbf{J}}_P(\boldsymbol{\theta}(k)) = \mathrm{I}[f(\boldsymbol{\theta}(k))]$. Additional measurements with independent measurement errors contribute extra terms to the sum in (36). The information bound for the parameter **θ**(*k*) imposed by a set of measurements is just the sum of the information matrix created by the prior before measurements plus the information matrix for each of the measurement vectors. The bound on the MSE is then calculated by inverting this matrix.

An important consideration for the use of bounds is how to account for the effect of measurements made at different time intervals on the lower bound of localization error. The use of measurements made at different times to track moving nodes is the basis of several proposed time-filtering location algorithms. These filtering algorithms include the Kalman filter (Chen, 1999, Hellebrandt and Mathar, 1999), the Extended Kalman Filter (Liu et al., 1998), and an extended version of the Interactive Multiple Model (IMM) filters (McGuire et al., 2003b).

Bounds on localization error with time filtering are dependent on a description of the time evolution of the node location using a model of the node motion. The location state of the node at sample interval k is given by $\mathbf{x}(k)$. For example, if the location state includes both the location and velocity of the mobile terminal, $\mathbf{x}(k)$ is then defined as $\mathbf{x}(k) = [p_x(k)\ v_x(k)\ p_y(k)\ v_y(k)]^T$ where $(p_x(k),p_y(k))$ is the terminal position at sample time k, where $(v_x(k), v_y(k))$ is the node velocity at sample time k. If the estimated location state for sample interval k given measurements up to sample interval k-d is denoted as $\hat{\mathbf{x}}(k \mid k-d)$, the estimation bound is denoted as

$$\tilde{\mathbf{P}}(k \mid k-d) \leq \mathrm{E}\left\{\left[\mathbf{x}(k) - \hat{\mathbf{x}}(k \mid k-d)\right]\left[\mathbf{x}(k) - \hat{\mathbf{x}}(k \mid k-d)\right]^T\right\}. \tag{37}$$

If the motion model is Markovian so that if $\mathbf{x}(k)$ is known then $\mathbf{x}(k+1)$ is independent of all $\mathbf{x}(k-d)$ for d>0, then the bound on the MSE of the filtering is given by (Šimandl et al. 2001):

$$[\tilde{\mathbf{P}}(k+1 \mid k+1)]^{-1} = [\tilde{\mathbf{P}}(k+1 \mid k)]^{-1} + \mathbf{L}_k^k, \text{ and} \tag{38}$$

$$[\tilde{\mathbf{P}}(k+1 \mid k)]^{-1} = \mathbf{O}_{k+1}^{k+1} - \mathbf{O}_{k+1}^{k,k+1}[\tilde{\mathbf{P}}(k \mid k)^{-1} + \mathbf{O}_{k+1}^{k}]\mathbf{O}_{k+1}^{k,k+1}. \tag{39}$$

The $\mathbf{O}$ matrices are defined as

$$\mathbf{O}_{k+1}^{k} = -\mathrm{E}\{\nabla_{\mathbf{x}(k)}[\nabla_{\mathbf{x}(k)} \ln f(\mathbf{x}(k+1) \mid \mathbf{x}(k))]^T\}, \tag{40}$$

$$\mathbf{O}_{k+1}^{k,k+1} = -\mathrm{E}\{\nabla_{\mathbf{x}(k+1)}[\nabla_{\mathbf{x}(k)} \ln f(\mathbf{x}(k+1) \mid \mathbf{x}(k))]^T\}, \tag{41}$$

$$\mathbf{O}_{k+1}^{k+1} = -\mathrm{E}\{\nabla_{\mathbf{x}(k+1)}[\nabla_{\mathbf{x}(k+1)} \ln f(\mathbf{x}(k+1) \mid \mathbf{x}(k))]^T\}, \text{ and } \mathbf{O}_{k+1}^{k+1,k} = [\mathbf{O}_{k+1}^{k,k+1}]^T. \tag{42}$$

The $\mathbf{L}_k^k$ is defined as

$$\mathbf{L}_k^k = -\mathrm{E}\{\nabla_{\mathbf{x}(k)}[\nabla_{\mathbf{x}(k)} \ln f(\mathbf{z}(k) \mid \mathbf{x}(k))]^T\} \tag{43}$$

with entries that can be taken from $\tilde{\mathbf{J}}_D(\boldsymbol{\theta}(k))$. If the motion model is a linear Markovian model with measurement and process noise given by independent Gaussian vector processes with no time dependencies then equations (38)-(43) will simplify down to the well known Ricatti equations for Kalman filters(Mendel 1995, Brookner, 1998). This derivation assumes that all the derivatives exist and all the expectations are bounded. The basic requirement is that the BCRB exists for localization error. If this condition is not satisfied, then more sophisticated bound calculations are required (Bobrovsky and Zakai, 1975; Kerr, 1989; Bobrovsky et al., 1990; Doerschuk, 1995; Tichavský et al., 1998, Van Trees and Bell, 2007). A recursion similar to (38)-(43) is also available for Weinstein-Weiss lower bounds (Rapoport and Oshman, 2004). These calculations are considerably more complex and well beyond the scope of this chapter.

EXAMPLES OF LOWER BOUND COMPUTATIONS

This section presents examples for calculation of the lower bound on two dimensional localization RMSE using ToA, TDoA, RSS, and AoA measurements. The bounds are calculated for a simple network scenario where the optimum Minimum Mean Square Error (MMSE) localization, $\hat{\boldsymbol{\theta}}(k) = \mathrm{E}[\boldsymbol{\theta}(k) \mid \mathbf{z}(k)]$ is available and easily calculated (Mendel, 1995). It is demonstrated that the Weinstein-Weiss and extended Ziv-Zakai bound calculations provide excellent measures of estimator performance for ToA, TDoA, AoA, and RSS measurements for two different base stations configurations with differing levels of GDOP. Bounds are also calculated for a mobile terminals located in a dense urban environment. The successful use of the localization accuracy bounds under NLoS radio propagation conditions for ToA and TDoA measurements is demonstrated. The last set of simulations demonstrate the use of the accuracy bounds to measure the accuracy of estimation possible for an actual indoor wireless sensor network using RSS measurements from an IEEE 802.11 WLAN base stations.

For the ToA, RSS, and AoA measurements, the measurement probability density function from (20) is assumed with the covariance given as $\mathbf{C} = \mathbf{I}^m \sigma^2$. The value of σ is varied to see the estimators' performance under different noise levels.

Bounds for a Simple Localization Scenario

The simulated network environment for the first three sets of localization is shown in Figure 2. For these simulations, the node locations are uniformly distributed within a disk of radius R_{area}. The node localization is performed from measurements made by $m=3$ base stations uniformly located on a circle of radius R_{BS} with the same center as the disc for the terminal locations. The local Cramér-Rao bound is not valid for this localization because of the existence of a prior probability density function for node location. The Cramér-Rao bound would give a bound on localization error only for localization performed without the use of prior information. The BCRB is not valid for this localization either because the finite support for the prior probability density function of the node location causes the regularity conditions of the bound to be violated.

Localization is performed based on RSS, ToA, or AoA measurements made by the base stations with the LoS propagation measurement model from (2). The first sets of simulations are ToA measurements performed with $R_{area} = R_{BS} = 15$m, which results in localization with low GDOP (Spirito, 2001). The RMSE for the ToA MMSE localization is compared with bounds calculated with the Ziv-Zakai and Weinstein-Weiss lower bound in Figure 3. It can be seen that the Ziv-Zakai lower bound provides the tightest bound to the optimal localization MMSE performance.

To show the danger of inappropriate use of the BCRB, the calculated BCRB bound values are also shown in Figure 3. The danger of the BCRB calculation is the calculations can still provide finite values, even though the bound is invalid, such as in this case. As can be seen in Figure 3, the BCRB MSE 'bound' exceeds the optimal MSE as the mean noise power increases. The BCRB calculations for each $\boldsymbol{\theta}(k)$ value use only the local curvature of $f(\mathbf{z}(k), \boldsymbol{\theta}(k))$ and do not include the boundary conditions. For the same reason, local Cramér-Rao bounds calculated near the boundaries of the region of support for $f(\boldsymbol{\theta}(k))$ are also invalid as they do not exclude estimated locations where $f(\boldsymbol{\theta}(k)) = 0$. The BCRB in this case is a lower bound on localization performed without use of the prior probability density function $f(\boldsymbol{\theta}(k))$ also known as Maximum Likelihood Estimation (Van Trees and Bell, 2007).

Figure 2. Simulation set-up

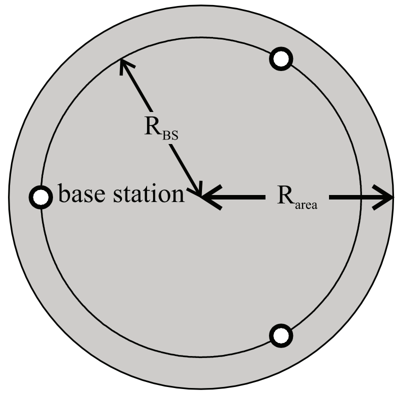

When R_{BS}=15 m for ToA location estimation, the posterior probability density function, $f(\boldsymbol{\theta}(k)\,|\,\mathbf{z}(k))$ is well approximated by a Gaussian probability density function for most values of $\mathbf{z}(k)$ which results in the Weinstein-Weiss bounds giving good approximations to the optimal MSE for low noise power. As the noise power increases, the effect of the boundary conditions on estimation increases and the Gaussian approximation to the posterior probability density function fails due to truncation at the boundary of the disc, causing the Weinstein-Weiss bounds to become loose with respect to the optimal MSE. However, the extended Ziv-Zakai bound, through its optimizations, is able to better incorporate the effect of boundary conditions which results in a better MSE bound for higher noise levels.

Simulations are performed with ToA measurements with R_{area} = 15m and R_{BS} = 5m which results in a higher GDOP than the previous simulation set for nodes located outside of the base station ring. The RMSE of the optimal MMSE localization and the Ziv-Zakai and Weinstein-Weiss lower bounds are shown in Figure 4. It can be seen that the Ziv-Zakai lower bounds is again tighter to the optimal localization performance than the Weinstein-Weiss lower bound. A comparison of Figure 3 and Figure 4 reveals that the Weinstein-Weiss lower bound is nearly identical for both of these sets. This shows that the Ziv-Zakai provides a better estimate of the lower bound in scenarios with localization with significant GDOP. For ToA location estimation when R_{BS}=5 m, the posterior probability density function is not well approximated as a Gaussian probability density function causing the performance of the Weinstein-Weiss bound to be loose with respect to the optimal MSE.

The last sets of simple localization scenario calculations were performed with LoS RSS propagation and LoS AoA measurements with R_{area} = 15m , R_{BS} = 5m, and α = 3. The results of the RMSE calculations are shown in Figure 5 and Figure 6. These results show that the Ziv-Zakai lower bound and the Weinstein-Weiss lower bound are fairly tight for RSS-based and AoA-based node localization errors as well as for the ToA localization errors. The poor approximation of $f(\boldsymbol{\theta}(k)\,|\,\mathbf{z}(k))$ as a Gaussian probability density function for RSS and AoA measurements is the chief explanation for the better performance of the extended Ziv-Zakai bound relative to the Weinstein-Weiss bound for these cases.

Bounds for Localization Error in a Dense Urban Environment

This section shows examples of the calculation for the Weinstein-Weiss lower bound calculation for the localization using ToA or TDoA measurements for street locations in a simulated dense urban en-

Figure 3. Terminal location with ToA measurements (R_{area} = 15 m, R_{BS}=15 m)

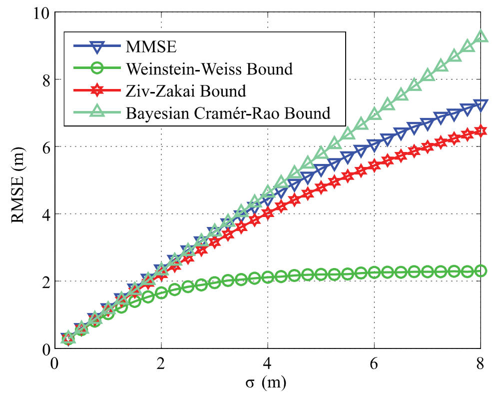

Figure 4. Terminal location with ToA measurements (R_{area}=15 m, R_{BS}=5 m)

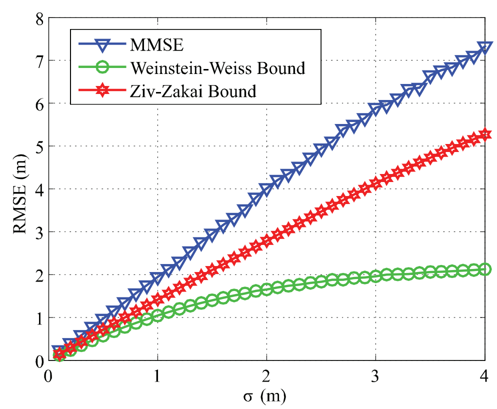

Figure 5. Terminal location with RSS measurements (R_{area}=15 m, R_{BS}=5 m)

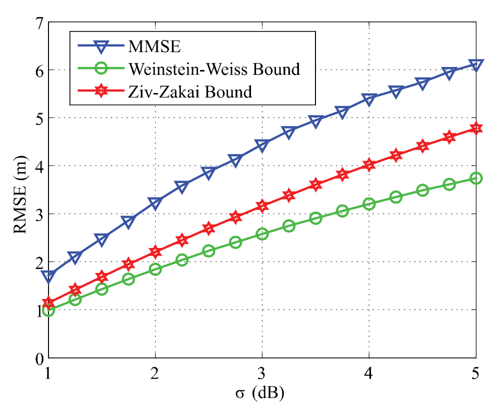

Figure 6. Terminal location with AoA measurements (R_{area}=15 m, R_{BS}=5 m)

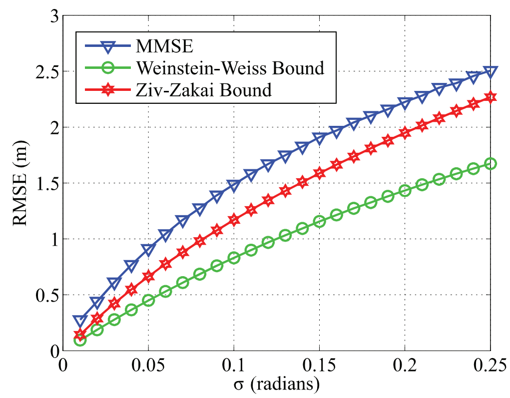

Figure 7. Dense urban environment

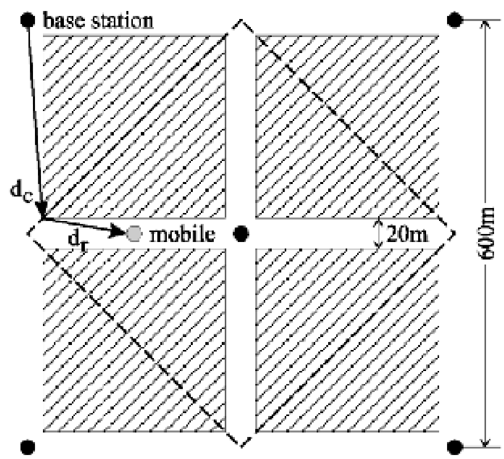

vironment, shown in Figure 7. Each street block is 300 m long with the streets being 20 m wide. The simulated node location is uniformly distributed over all street locations. The node is localized with measurements obtained from the m = 3 nearest base stations to the mobile terminal. Radio propagation is either LoS or NLoS with the building blocking the LoS propagation path if the shortest distance straight line path between the node and the measuring base stations passes through a building block. In this case, the signal diffracts around corners with the noise free propagation distance for a single base station being d_C+d_r as seen in Figure 7.

The RMSE results for the approximate MMSE localization from (McGuire et al., 2003a) using ToA and TDoA measurements in this environment are compared with the Weinstein-Weiss lower bound in Figure 8. For TDoA measurements, the nearest base station is used as the reference base station. These results show that the Weinstein-Weiss lower bound is fairly tight to the actual localization error performance. These results also show that excellent localization accuracy performance is available for the case when NLoS radio propagation is occurring, since when the 3 nearest base stations measurements are used for localization, only the nearest base station has LoS propagation with the other two measuring base stations experiencing NLoS propagation. Note that localization error from TDoA measurements

Figure 8. Weinstein-Weiss lower bound calculations

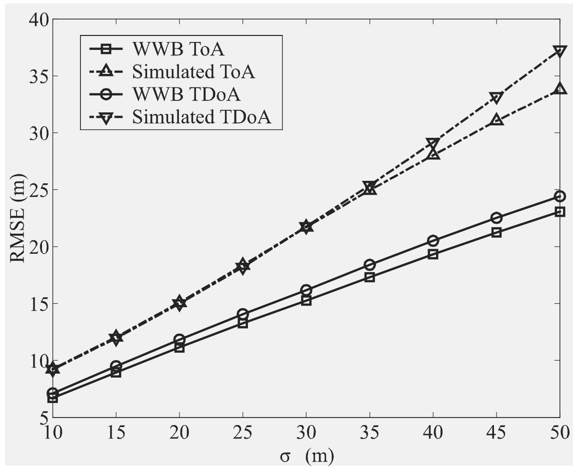

Figure 9. RSS survey set bound calculation

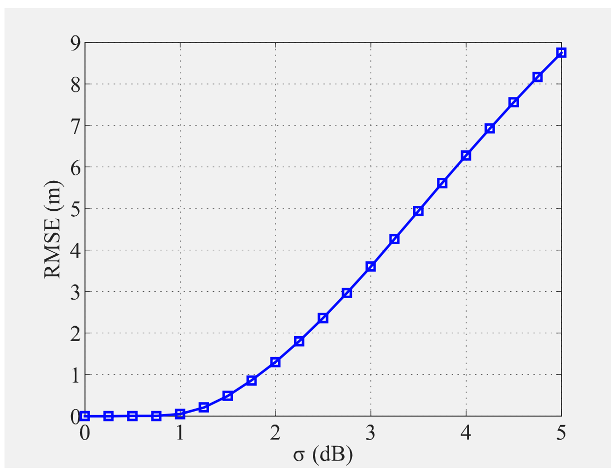

is slightly worse than the ToA localization error. This is due to the fact that the TDoA measurements contain less information than ToA measurements since the full TDoA measurement vector can be calculated from the ToA measurement vector but not vice versa(Shin and Sung 2002).

Survey Set Estimation Lower Bound

In this section, the results of the calculations for the lower bound on the localization RMSE based on an estimator constructed from survey points is presented. For this experiment, RSS survey measurements were collected for each of the 117 seat locations of a 10 m by 13 m lecture hall at the University of Victoria in British Columbia, Canada. At each location, the RSS from 12 of the IEEE wireless local area network base stations for the engineering network were recorded. It should be noted this is a pure

NLoS propagation environment since none of these base stations are located in the lecture hall, and only 3 base stations are located on the same floor as the lecture hall.

The bound on the estimation RMSE for different standard deviations of the measurement noise is shown in Figure 9. The actual standard deviation for the measurement noise for the RSS measurements was 2.1 dB with the resulting RMSE of the estimated location being 2.7 m and the bound on the RMSE is 1.49 m. This shows that the bound is fairly tight to the localization error.

CONCLUSION

This chapter has presented several methods for calculating performance bounds for node localization in wireless sensor networks. These bounds account for information available on the node location from the sensor selection process and consider complicating effects such as radio propagation including both LoS and NLoS propagation paths within the network environment. It is also demonstrated how these bounds can be used to determine the location accuracy available from a given survey set.

Several bounds on localization error have been presented. When the prior probability density function for node location has infinite support and there is only LoS propagation in the network area, the Bayesian Cramér-Rao bound on the localization error is valid. This bound requires only a simple addition of two information matrices, each calculated via simple expectations. However, the Bayesian Cramér-Rao lower bound becomes invalid when either the prior probability density function of the node location has only finite support or the wireless sensor network's environment contains both LoS and NLoS radio propagation. The chapter presents two bounds to handle these cases, the Weinstein-Weiss bound and the extended Ziv-Zakai lower bound. The Weinstein-Weiss lower bound is the easiest to apply, calculated from expectations of functions derived from the measurement and location densities with the optimization performed with respect to a single scalar parameter. The extended Ziv-Zakai bound is calculated from expectations but optimization is performed with respect to a vector of parameters requiring considerably more computational effort.

REFERENCES

Bell, K. L., Steinberg, Y., Ephraim, Y., & Van Trees, H. L. (1997). Extended Ziv–Zakai lower bound for vector parameter estimation. *IEEE Transactions on Information Theory*, *43*(2), 624-637.

Bobrovsky, B. Z., & Zakai, M. (1975). A lower bound on the estimation error for Markov processes. *IEEE Transactions on Automatic Control*, *20*(6), 785-788.

Bobrovsky, B. Z., Zakai, M., & Kerr, T. H. (1990). Comments on Status of CR-like lower bounds for nonlinear filtering. *IEEE Transactions on Aerospace and Electronic Systems*, *26*(5), 895-898.

Botteron, C., Fattouche, M., & Høst-Madsen, A. (2004). Cramer–Rao Bounds for the Estimation of Multipath Parameters and Mobiles' Positions in Asynchronous DS-CDMA Systems. *IEEE Transactions on Signal Processing*, *52*(4), 862-875.

Brookner, E. (1998). *Tracking and Kalman filtering made easy*. Toronto, ON: John Wiley & Sons.

Caffery, J. J., & Stüber, G. L. (1998). Overview of radiolocation in CDMA cellular systems. *IEEE Communications Magazine*, *36*(4), 38-45.

Chen, P.-C. (1999). A cellular based mobile location tracking system. *In Proceedings of the IEEE Vehicular Technology Conference* (pp. 1979-1983), Houston, TX, USA.

Doerschuk, P. C. (1995). Cramer-Rao bounds for discrete-time nonlinear filtering problems, *IEEE Transacations on Automatic Control*, *40*(8), 1465-1469.

Federal Communications Commission. (2006). *FCC Docket 94-102: Report and order and further notice of proposed rulemaking in the matter of revision of the commission's rules to ensure compatibility with enhanced 911 emergency calling systems*.

Duda, R. O., Hart, P. E., & Stork, D. G. (2001). *Pattern Classification*. Second Edition, Toronto, ON: John Wiley & Sons.

Hellebrandt, M., & Mathar, R. (1999). Location tracking of mobiles in cellular radio networks. *IEEE Transactions on Vehicular Technology*, *48*(5), 1558-1562.

Kay, S. M. (1993). *Fundamentals of Statistical Signal Processing: Estimation Theory*. Upper Saddle River, NJ: Prentice Hall.

Kerr, T. H. (1989). Status of CR-like lower bounds for nonlinear filtering. *IEEE Transactions on Aerospace and Electronic Systems*, *25*(5), 590-600.

Kim, W., Jee, G.-I., & Lee, J. G. (2001). Wireless location with NLOS error mitigation in Korean CDMA system. In *Proceedings of the Second International Conference on 3G Mobile Communication Technologies* (pp. 134-138). London, U.K.

Leon-Garcia, A. (1994). *Probability and Random Processes for Electrical Engineering*. Second Edition, Don Mills, Ontario: Addison-Wesley Publishing Company.

Liu, T., Bahl, P., & Chlamtac, I. (1998). Mobility modeling, location tracking, and trajectory prediction in wireless ATM networks. *IEEE Journal on Selected Areas in Communications*, *16*(6), 922-936.

Mendel, J. M. (1995). *Lessons in Estimation Theory for Signal Processing, Communications, and Control*. New Jersey: Prentice-Hall.

McGuire, M., Plataniotis, K. N. & Venetsanopoulos, A. N. (2003a) Location of mobile terminals using time measurements and survey points. *IEEE Transactions on Vehicular Technology*, *52*(4), 999-1011.

McGuire, M., & Plataniotis, K. N. (2003b). Dynamic model-based filtering for mobile terminal location estimation. *IEEE Transactions on Vehicular Technology*, *52*(4), 1012-1031.

Patwari, N., Hero, A. O., Perkins, M., Correal, N. S., & O'Dea, R. J. (2003). Relative location estimation in wireless sensor networks. *IEEE Transactions on Signal Processing*, *51*(8), 2137-2148.

Ray, S., Lai, W., & Paschalidis, I. C. (2006). Statistical location detection with sensor networks, *IEEE Transactions on Information Theory*, *52*(6), 2670-2683.

Qi, Y., & Kobayashi, H. (2002). Cramér-Rao lower bound for geolocation in non-line-of-sight environment. In *Proceedings of the 2002 IEEE International Conference on Acoustics, Speech, and Signal Processing*, *3*, 2473-2476.

Rapoport, I., & Oshman, Y. (2004). Recursive Weiss-Weinstein lower bounds for discrete-time nonlinear filtering. *In Proceedings of the 43rd IEEE Conference on Decision and Control*, *3*, 2662-2667).

Rife, D. C., Goldstein, M., & Boorstyn, R. R. (1975). A unification of Cramér-Rao type bounds. *IEEE Transactions on Information Theory*, *IT-21*(3), 330-332.

Sheu, J.-P., Li, J.-M., & Hsu, C.-S. (2006). A distributed location estimating algorithm for wireless sensor networks. *In Proceedings of the IEEE International Conference on Sensors Networks, Ubiquitous, and Trustworthy Computing* (pp. 218-225).

Shin, D.-H., & Sung, T.-K. (2002) Comparisons of error characteristics between TOA and TDOA Positioning. *IEEE Transactions on Aerospace and Electronic Systems*, *38*(1), 307-311.

Šimandl, M., Královec, & Tichavský, P. (2001). Filtering, predictive, and smoothing Cramér-Rao bounds for discrete-time nonlinear dynamic systems. *Automatica*, *37*(11), 1703-1706.

Spirito, M. A. (2001). On the accuracy of cellular mobile station location estimates. *IEEE Transactions on Vehicular Technology*, *50*(3), 674-685.

Steele, R. (1992). *Mobile Radio Communications*. Piscataway, NJ: IEEE Press.

Tekinay, S., Chao, E., & Richton, R. (1998). Performance benchmarking for wireless location systems. *IEEE Communications Magazine*, *36*(4), 72-76.

Tichavský, P., Muravchik, C. H., & Nehorai, A. (1998). Posterior Cramér-Rao bounds for discrete-time nonlinear filtering. *IEEE Transacations on Signal Processing*, *46*(5), 1386-1396.

Torrieri, D. J. (1984). Statistical theory of passive location systems. *IEEE Transactions on Aerospace and Electronic Systems*, *AES-20*(2), 183-198.

Van Trees, H. L. (2001). *Detection, Estimation, and Modulation Theory*. Volume I, Toronto, Ontario: John Wiley & Sons.

Van Trees, H. L., & Bell, K. L. (Ed.) (2007). *Bayesian Bounds for Parameter Estimation and Nonlinear Filtering/Tracking*. Piscataway, NJ: IEEE Press.

Weinstein, E., & Weiss, A. J. (1988). A general class of lower bounds in parameter estimation. *IEEE Transactions on Information Theory*, *34*(2), 338-342.

Wylie, M. P., & Holtzman, J. (1996). The non-line of sight problem in mobile location estimation. In *Proceedings of the International Conference on Universal Personal Communications* (pp. 827-831), Cambridge, MA, USA.